

Ethylene-Propylene Copolymer Aggregation in Selective Hydrocarbon Solvents

M. J. Kucks and H. D. Ou-Yang*

Department of Physics and Center for Polymer Science & Engineering, Lehigh University, Bethlehem, Pennsylvania 18015

I. D. Rubin

Texaco R & D Department, P.O. Box 509, Beacon, New York 12508

Received October 7, 1992; Revised Manuscript Received April 26, 1993

ABSTRACT: Intrinsic viscosity measurements of 80–20 molar ratio ethylene-propylene (EP) copolymers in selective solvents have shown a dramatic decrease in viscosity when temperature was lowered from 50 to –10 °C. In this study we show that both chain association and cluster contraction can occur. Viscometry, dynamic light scattering (DLS), and static light scattering (SLS), including Zimm plots, were used to examine the number of polymer chains in the aggregated clusters and the cluster size of a 322 000 molecular weight EP copolymer in methylcyclohexane (MCH) and tetralin (THN). For all temperatures and concentrations studied the polymer formed aggregated clusters. However, in MCH (the better solvent) the polymer volume fraction, from viscometry, maintained a constant value over temperature whereas in THN (the poorer solvent) the polymer volume fraction dropped by a factor of 5 as the temperature was lowered to –10 °C. Thus, while both systems formed aggregated clusters, the solvent quality determined the microstructure which caused this temperature-sensitive viscosity behavior. Although all data showed polymer aggregation, higher values were obtained for the average number of chains in the clusters by a combination of viscometry and DLS than by SLS.

Introduction

Ethylene-propylene (EP) copolymer is used as a viscosity-modifying additive in motor oils. One of the properties of interest is its ability to enhance base oil viscosity more at high temperatures than at low temperatures. This performance counteracts the loss of base oil viscosity as engine temperatures increase without excessively increasing viscosity at low temperatures.^{1,2} In spite of its wide use, little has been reported on the conformational changes and aggregation that occur as temperature is varied for concentrations above those used to measure intrinsic viscosities. Mays *et al.* measured the intrinsic viscosities of 50–50 alternating EP copolymer in hydrocarbon solvents from 5 to 40 °C to determine the temperature coefficient of the unperturbed single-chain polymer.³ A performance comparison between 50–50 EP copolymer in a commercially available base oil and other viscosity improvers has been made by Maderek *et al.* Measurements were made of the intrinsic viscosity, kinematic viscosity, viscosity index, and activation energy from 40 to 100 °C.⁴ Filiatrault *et al.* measured intrinsic viscosities at 25 °C to determine the effect of polymer-solvent orientation correlations.^{5–8} Recent work by Rubin *et al.*^{2,9–10} showed that the intrinsic viscosity of an 80 mol % ethylene, 322 000 MW copolymer dropped well below the intrinsic viscosity of a 60 mol % ethylene, 148 000 MW copolymer at –10 °C. In contrast, the 80% copolymer had an intrinsic viscosity of twice the 60% copolymer at 50 °C. This behavior was observed only in the poor solvent tetralin (THN). In the better solvent, methylcyclohexane (MCH), the polymer showed no drop in intrinsic viscosity at low temperatures.⁹ The unanswered question is what microstructural changes occur to cause this different viscosity behavior? The individual polymer chains may contract, thereby reducing the hydrodynamic volume. Or, there may be polymer aggregation, along with contraction, which would reduce the number density as well as the hydrodynamic volume. To answer this question, we studied the same 80% ethylene–20% propylene copolymer

in MCH and THN by viscometry, dynamic light scattering (DLS), and static light scattering (SLS) techniques. Our data were combined with the molecular weight determined by Rubin to obtain the degree of aggregation of the polymer and the polymer density in the aggregates.

Experimental Section

The copolymer used consisted of randomly distributed ethylene and propylene monomers in a linear chain. The weight-average molecular weight, $M_w = 322\,000$, was determined in 1,2,4-trichlorobenzene at 130 °C, conditions at which no aggregation is expected, in a Waters 150C GPC unit. Polydispersity was 4.1 [(weight average)/(number average) molecular weight]. NMR analysis showed that the chains consisted of 80 mol % ethylene, where 65% of the ethylene segments contained three or more contiguous ethylene monomers. The average number of contiguous ethylene monomers within this 65% was 6.1. X-ray scattering showed that solid EP copolymer contains a crystallinity of 5.2%. According to Rubin *et al.*, who performed the analysis and designated this polymer EP5,⁹ this was attributed to these relatively long ethylene sequences.

A 1.000 wt % stock solution of the polymer was made in 99% pure MCH from Fisher by dissolving it at 80 °C under a nitrogen blanket with gentle agitation. This stock was passed through a binderless glass microfiber filter. Gravimetric analysis showed that polymer retention by the filter was negligible. When a similar filtering was attempted on 1.000 and 0.020 wt % stock solutions of the polymer in THN at room temperature, the filter clogged after passing several milliliters of solution. This confirmed that MCH was a better solvent than THN. Half of the polymer from the filtered MCH stock was recovered in a vacuum oven at 60 °C and redissolved in filtered 99% pure THN from Aldrich to 1.000 wt % concentration. Final concentrations were made by dilution with filtered solvent. The 0.100% solutions were placed in a freezer at –15 °C for 48 h to fully equilibrate before temperature-dependent measurements were made. They were allowed to soak for a minimum of 2 h at each temperature tested from –10 to 40 °C. All samples used in the concentration-dependent study were equilibrated at the temperature extremes for at least 48 h before testing.

Viscosity measurements were made on a Zimm viscometer^{11,12} in which an aluminum rotor was weighted to float in the test solutions. Torque was applied to this floating rotor via a rotating

permanent magnet located outside a thermal jacket which held the test solution. A thermobath circulator provided 0.1 °C temperature control. Measurements at low constant shear rates (10–20 s⁻¹) made this a better choice than a capillary viscometer for comparing the viscometric and light scattering data. Volume fractions were calculated using the Einstein equation: $\phi = \eta_{sp}/2.5$,¹³ where ϕ is the polymer volume fraction and η_{sp} is the specific viscosity. Since hydrodynamic interactions are ignored, the volume fractions obtained from this analysis should be viewed as maximum possible values.

The dynamic light scattering correlation function was collected on a Brookhaven BI-200SM goniometer connected to a BI2030AT digital correlator. The light source consisted of a 35-mW Spectra-Physics Model 127 He-Ne laser. Temperature was controlled to 0.1 °C. Data analysis consisted of fitting this correlation function to a second-order cumulant form.¹⁴ From this fitting we extracted a value for the translational diffusion constant, D , which is inversely related to the average polymer hydrodynamic radius, R_h , through the Stokes-Einstein relation, $D = kT/(6\pi\eta R_h)$.¹⁴ Data were collected at a scattering angle of 45°.

Static light scattering (SLS) data were also collected using the Brookhaven BI-200SM goniometer. For polymer aggregates whose size is an appreciable fraction of a laser wavelength the measured time-averaged intensity is modulated by interference effects from light scattered by different parts of the cluster. By taking data at small angles (<40°), it is possible to extrapolate the data to a zero-angle scattered intensity which is insensitive to the interference effects caused by large particles. This intensity is directly related to the mass of the scattering particle. SLS data were collected over angles from 15° to 150°. Where scattered intensities were too high to be detected without damage to the PMT, neutral density filters were used to reduce the incident laser intensity to an acceptable level. The degree of attenuation was measured each time a filter was used, and final intensity values were normalized to the same incident laser intensity and pinhole size (1 mm).

Zimm plots were made according to the equation:¹⁴

$$KC/\Delta R = (1/M + 2A_2C)[1 + B\langle R_g^2 \rangle \sin^2(\theta/2)] \quad (1)$$

where $K = k^4 n_0^2 (dn/dc)^2 / (4\pi^2 N_A)$ (where k is the wavenumber, n_0 the solvent refractive index, and dn/dc the refractive index increment), ΔR is the excess Rayleigh ratio, C the concentration, M the scatterer molecular weight, and A_2 the second virial coefficient. Also, $B = (4/3)k^2 \langle R_g^2 \rangle$ is the mean-square radius of gyration, and θ is the scattering angle. In this study A_2C was assumed small compared with $1/M$ and the data for $\theta = 0$ were used, which left the simplified equation: $M = \Delta R/(KC)$. Inclusion of the A_2 term would only make the calculated mass larger, and so the reported figures should be viewed as minimum possible values. The refractive index increment was measured on an LDC refractometer using several concentrations of the polymer in MCH ranging from 0.020% to 0.200% by weight. The data were linear over this range and gave a value of $dn/dc = 0.057$ mL/g. This same value was used in the analysis of the THN samples.

Data Analysis and Discussion

(A) Analysis. The critical overlap concentration of a polymer solution marks the onset of the semidilute regime where data analysis becomes much more difficult. The critical concentration for our systems was calculated using $C^* = \nu M_w / N_A V_g$, where ν is the aggregation number, M_w is the polymer weight-average molecular weight, N_A is Avogadro's number, and V_g is the average hydrodynamic cluster volume. If our system were unaggregated ($\nu = 1$) and the solvent quality were good, the theoretical critical concentration for our copolymer would be 0.100% by weight. But, because of polymer aggregation and contraction all samples were below their critical concentration.

We used a method similar to that proposed by Flory and Mandelkern for the determination of mass from viscometry and sedimentation velocity data.¹⁵ However, instead of using sedimentation velocity, we used DLS to determine the hydrodynamic radius, R_h . Measurements of specific viscosity gave the polymer volume fraction using

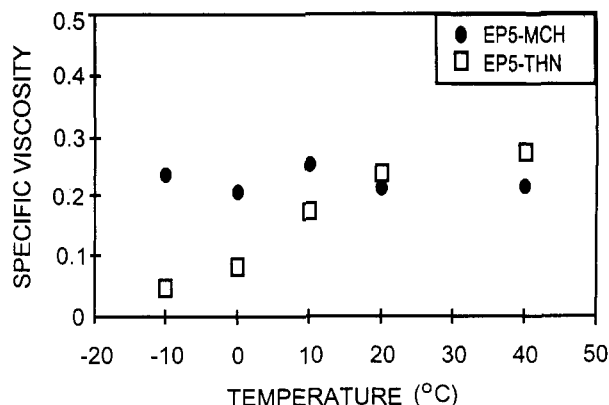


Figure 1. Specific viscosity versus temperature for EP5 in methylcyclohexane (MCH) and tetralin (THN) at 0.100%. Viscosity enhancement is flat over temperature in MCH and drops by a factor of 5 from 40 to -10 °C in THN.

the Einstein equation: $\eta_{sp} = 2.5\phi$. Since we know the concentration, C , the average density of the solvated polymer in the cluster can be calculated as $\langle \rho \rangle \cong C/\phi$. DLS was used to determine the hydrodynamic volume of the polymer cluster: $V_h = (4/3)\pi R_h^3$. Average cluster mass was then calculated as $\langle M \rangle \cong \langle \rho \rangle V_h$. We determine the aggregation number, ν , by the relation $\nu = \langle M \rangle / (M_w/N_A)$. Independently, we can also determine ν from the zero-angle intensity using static light scattering, as shown below.

(B) Viscometry. Since Rubin *et al.* gave ample verification of the temperature-dependent viscosity performance of this copolymer in these same two solvents by measuring intrinsic viscosity, we measured the specific viscosity at only one concentration, 0.100%. This was done at several temperatures covering the range from -10 to 40 °C. As pointed out previously, this concentration is just at the theoretical critical concentration if all coils are unaggregated and in a good solvent. It was reasoned that any aggregation effects would be quite prominent in this region, and light scattering intensities were high enough to give good signal to noise ratios for DLS and SLS at all temperatures.

Since the characteristic ratio for both polyethylene and polypropylene is 6.8,¹⁶ the length of the statistical element for our copolymer may be estimated as 1.2 nm. The radius of gyration is given by $R_g = (a/6^{1/2})N^{3/5}$ in a good solvent and $R_g = (a/6^{1/2})N^{1/2}$ in a θ solvent, where a is the length of the statistical element and N is their number.¹⁷ Since viscosity is a hydrodynamic effect, we used the hydrodynamic radius instead of the radius of gyration to calculate the expected specific viscosity. With the hydrodynamic radius $R_h = R_g/1.3$,¹⁴ we have $R_h = 40$ nm and $R_h = 19$ nm, in good and θ solvents, respectively. Thus, isolated coils of our copolymer at 0.100% would be expected to have specific viscosities of 1.2 in good solvents and 0.13 in θ solvents.

Figure 1 shows specific viscosity data for this polymer in both MCH and THN at a shear rate of 15 s⁻¹, where shear deformation of the polymer was expected to be negligible. Both solutions had specific viscosities at 40 °C that were only one-fourth of the predicted values for single polymers in a good solvent. However, they were two and a half times the predicted value for polymers in a θ solvent. Thus, the cohesion of the ethylene sequences seems to contract the chains below the extension expected in a good solvent medium.

As temperature was reduced, the viscosity of the MCH solution did not change while for the THN solution it decreased by a factor of 5. This behavior in THN can be caused by either chain contraction or precipitation. Gravimetric analysis of the top fraction of the sample

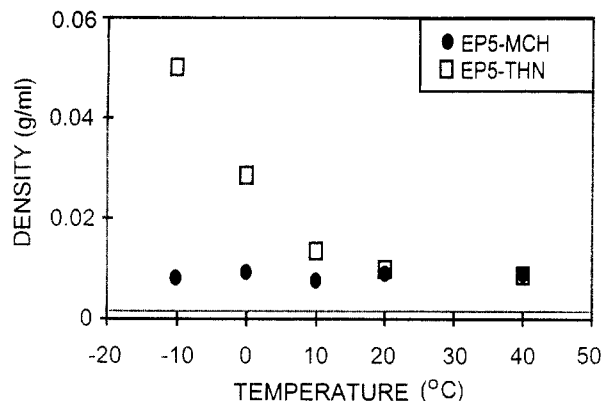


Figure 2. Polymer aggregate density versus temperature from viscometry. Density increases at lower temperatures in tetralin (THN) and remains constant in methylcyclohexane (MCH). The dashed line shows the calculated density of a single Gaussian coil in a good solvent.

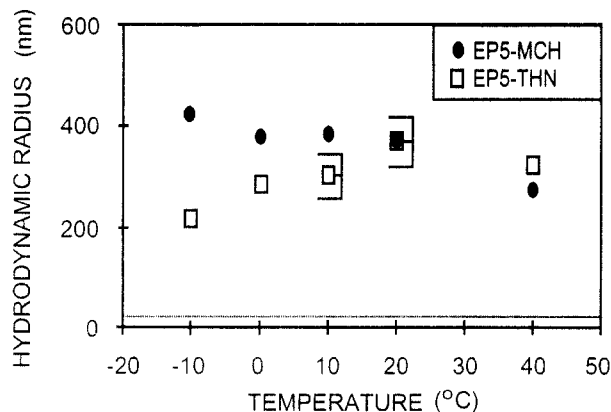


Figure 3. Hydrodynamic radius versus temperature from dynamic light scattering at 0.100%. The dashed line shows the hydrodynamic radius of single coils that would give rise to the measured specific viscosity at room temperature. The data clearly show that polymers are aggregated at all temperatures.

showed no evidence of precipitation after 48 h of soak at -10°C . Average polymer density was calculated as $\langle \rho \rangle = 2.5C/\eta_{sp}$. Figure 2 shows these densities for both solutions at all temperatures tested. They were all higher than expected for single Gaussian chains in a good solvent (indicated by the dashed line at 0.1 g/dL).

(C) Dynamic Light Scattering. If one assumes that the polymers were unaggregated monodisperse coils, it is possible to calculate the hydrodynamic radius from the measured specific viscosity shown on Figure 1. To produce a specific viscosity of 0.24 at a concentration of 0.100% by weight would require single coils with $R_h = 25$ nm. Figure 3 shows the results of DLS measurements. At all temperatures the radii were at least an order of magnitude larger than 25 nm. Thus, the polymers in both solutions were in an aggregated state at all temperatures. These data represent two independent measurements with various soak times (ranging from 3 to 12 h) at each temperature at a scattering angle of 45° . The "error bars" indicate the measured extremes from these two data sets, and the data points are simply the average of these extremes. Where no "error bars" are shown, the results from both tests were comparable. Polydispersity was 40–50% of the measured radii, which indicates that the results from both tests were consistent within this range. The cumulant analysis algorithm used to determine the hydrodynamic radius makes no correction for any assumed particle size distribution. Thus, the low angle used in DLS measurements weighted the particle sizes in favor of the larger radii. Therefore, the radii given in Figure 3 should be viewed as maximum possible values.

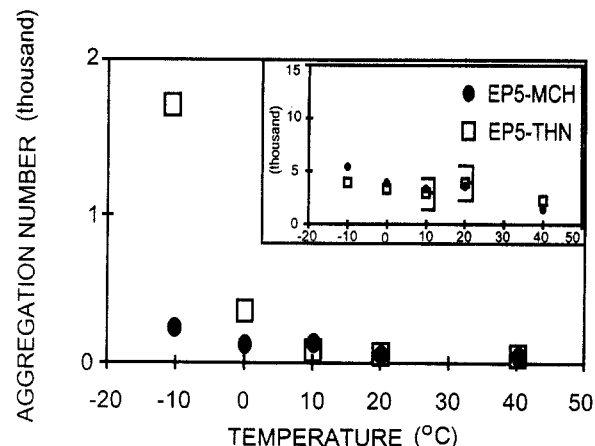


Figure 4. Aggregation number versus temperature as measured from SLS absolute intensities at zero angle at 0.100%. Aggregation is similar in each solvent at 40°C and is 10 times higher in THN than MCH at -10°C . Inset: Shows the scatterer aggregation numbers determined from DLS-viscometry data. For all temperatures the SLS aggregation numbers are less than the DLS-viscometry values. However, both show highly aggregated structures at -10°C .

The inset plot of Figure 4 shows the average aggregation number per cluster determined by combining viscometry and DLS and dividing the cluster weight arrived at by the M_w . This was compared with the independent evaluation of aggregation number from SLS zero-angle intensities, shown in the main plot of Figure 4, using eq 1 (as described in the next section). Aggregation numbers obtained by SLS were consistently lower than those obtained by viscometry and DLS, with the better agreement occurring at -10°C and the discrepancy increasing with temperature. The fact that DLS seemed insensitive to changes in aggregation number with temperature may be understood as the existence of a relatively few large scatterers at all temperatures which dominate the correlation function at the 45° scattering angle. Thus, while many aggregates may have been breaking up with increased temperature, as indicated by SLS, the average value determined from the cumulant fitting of the correlation function remained relatively constant. To obtain better consistency, measurements of DLS data at several different scattering angles are in progress. The SLS analysis, since it involves fitting the intensity data over a range of scattering angles, provides a better picture of the aggregation process and how it changes with temperature.

In the main plot of Figure 4 the degree of aggregation at the lowest temperature was an order of magnitude greater in THN than in MCH while at the higher temperatures it was virtually the same in both solvents. This indicates that solvent quality was similar at higher temperatures and that THN became a poor solvent more rapidly with reduced temperature than did MCH. Figures 5 and 6 show the effect of solvent quality on the hydrodynamic radius of these aggregates over a range of solution concentrations. Figure 5 indicates that in THN the aggregate radius was lower at -10°C than at 50°C , even though the aggregation number increased. In contrast, Figure 6 indicates that in MCH the aggregate radius at -10°C was almost twice that at 50°C . This contraction in THN caused the drop in viscosity shown on Figure 1 at low temperatures.

There are no data shown at the two lowest concentrations in either solvent at 50°C because there was not enough scattered intensity to allow a measurement with DLS. The signal to noise ratio was virtually zero for these low concentrations, indicating that the scatterer mass was extremely low. However, at -10°C , the signal to noise

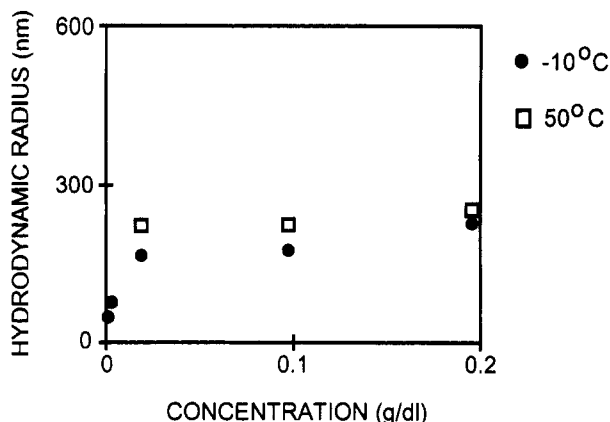


Figure 5. Hydrodynamic radius vs concentration for EP5 in THN at -10 and 50 °C. The radius dropped at the lower temperature.

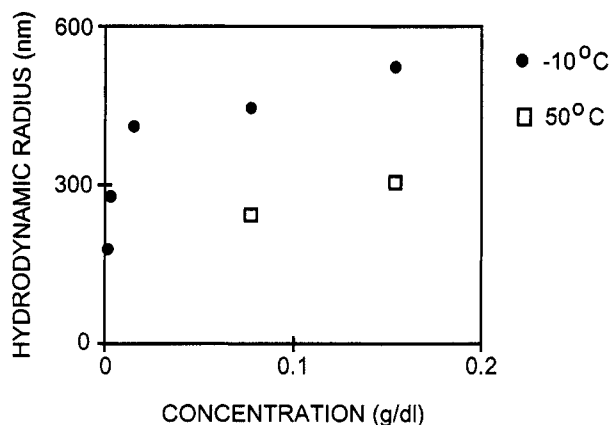


Figure 6. Hydrodynamic radius vs concentration for EP5 in MCH at -10 and 50 °C. The radius increased at the lower temperature.

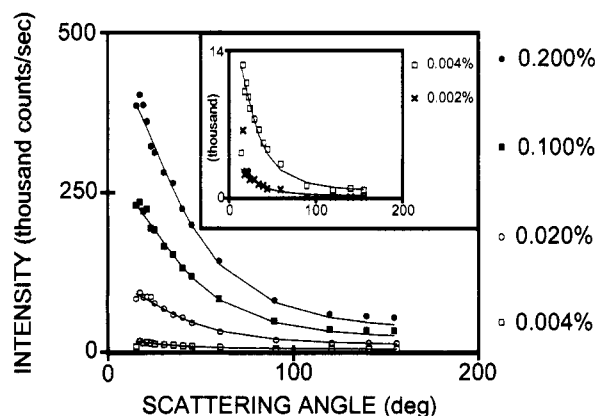


Figure 7. Scattered light intensity vs scattering angle for EP5 in THN at several concentrations at 50 °C. The intensity rises linearly with concentration, so the scatterer mass is constant.

ratio was such that good DLS measurements could be made, indicating that the scatterer mass had increased substantially. Because of the size distribution problems mentioned above for DLS, these plots only show a quantitatively different response to changes in temperature for the copolymer in these two solvents. To determine actual aggregation numbers with more certainty, the SLS data were used.

(D) Static Light Scattering. Static light scattering data were evaluated in two complementary ways. First, the absolute scattered intensity as a function of scattering angle was plotted and fitted to either a solid sphere or Gaussian form factor, depending on which one gave a better fit at low angle (Figure 7). This fitting provided an extrapolated zero-angle intensity from which a molecular

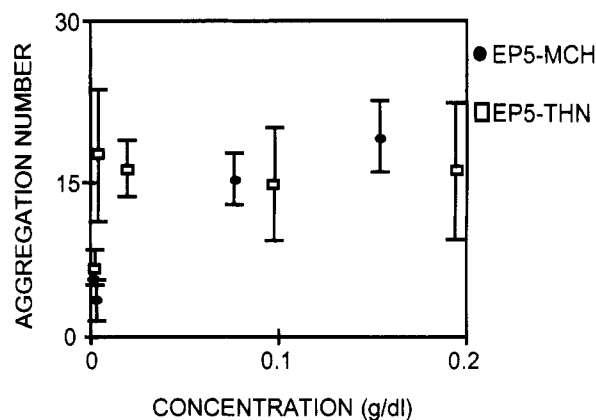


Figure 8. Aggregation number vs concentration of EP5 in MCH and THN at 50 °C. Aggregation numbers are the same in each solvent.

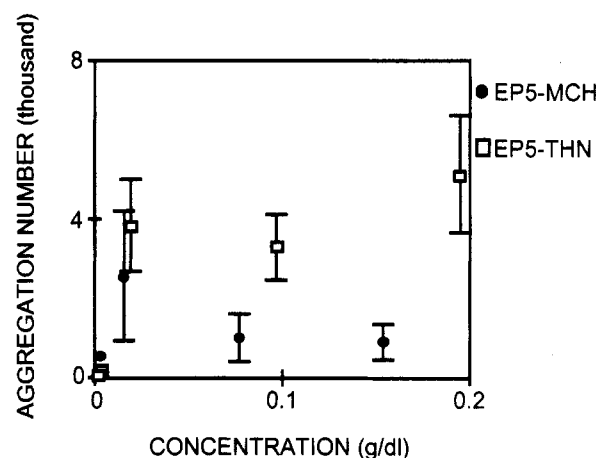


Figure 9. Aggregation number vs concentration of EP5 in MCH and THN at -10 °C. Aggregation in THN is more prominent than in MCH.

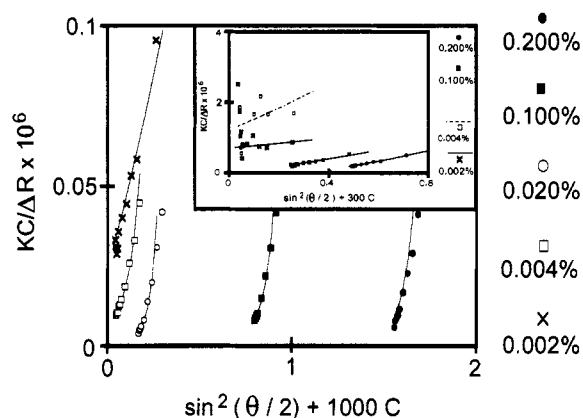


Figure 10. Zimm plot of EP5 in MCH at -10 °C. Inset: 50 °C.

weight was calculated using eq 1. Dividing this mass by the weight-average molecular weight gave the degree of aggregation, as shown in Figures 8 and 9. Zimm plots (Figures 10 and 11) were also made since these gave a qualitative evaluation of the degree of aggregation as concentration was varied. By comparing different plots, an evaluation of how aggregation changed with temperature and solvent was also possible. In all plots the solids lines show the fitting function and the markers show the actual data.

Figure 7 shows the actual scattered photon counts per second as a function of scattering angle for EP5 in THN at 50 °C at several concentrations. The inset shows the lowest two concentrations in more detail. This plot is typical of the data collected for the copolymer in THN

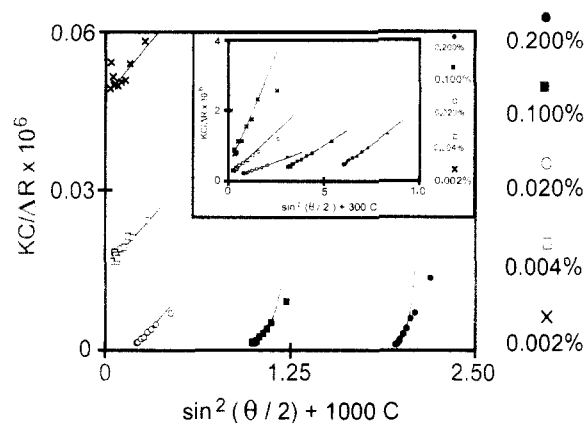


Figure 11. Zimm plot of EP5 in THN at -10°C . Inset: 50°C .

and MCH at the temperature extremes (-10 and 50°C) at these concentrations. The data show that the intensity increased with concentration, as expected. If this increased intensity were linear in concentration, it would simply be due to the greater number of scatterers per unit volume and the scatterer mass would be constant. If there is an increase beyond that which is linear in concentration, then it is attributable to an aggregation process. The zero-angle intensity at 0.002% was 5000 counts per second (cps) and the intensity at 0.200% was 500 000 cps. For this sample the increase in intensity with concentration was linear. No relative aggregation with concentration is evidence. However, zero-angle intensity analysis showed that the scatters were 10 times more massive than the molecular weight found by Rubin. Figures 8 and 9 show these absolute aggregation numbers for each concentration in MCH and THN, where Figure 8 is for the 50°C temperature and Figure 9 is for -10°C .

A Zimm plot is a convenient way to show the low-angle scattering data at several concentrations. It allows an easy evaluation of aggregation since, according to eq 1, the concentration dependence of the scattering intensity is normalized. Thus, any changes in the zero-angle $KC/\Delta R$ values at different concentrations are inversely related to changes in scatterer mass. Figures 10 and 11 show Zimm plots for MCH and THN samples, respectively. The inset shows the data for 50°C while the main plot is for -10°C . Both insets show a very slight increase in molecular weight with increased concentration (a factor of 3 or 4), but the lowest concentration and next highest concentration data on Figure 10 are inverted in their positions on the plot. This is due to the low signal to noise ratio of the scattering data at this temperature. The main plots in Figure 10 shows that the polymer in MCH solution was still aggregating by a factor of 3 or 4 with increased concentration at -10°C . However, the absolute value of $KC/\Delta R$ indicates that the mass increased by a factor of 25–50 in going from 50 to -10°C . By contrast, the THN sample at -10°C (main plot, Figure 11) shows a factor of 200 increase in aggregation with concentration, with the largest increase occurring for the two lowest concentrations. The absolute value of $KC/\Delta R$ indicates that in going from 50 to -10°C the aggregation increased by a factor of 100–200. By comparing the inset plots, one can see the effect of changing the solvent at 50°C was minimal. Both sets of data look similar. However, the main plots show the effect of changing solvent at -10°C was very dramatic. Aggregation with increased concentration was much more pronounced in the THN sample than in MCH. This increased tendency to aggregate at low temperatures in THN, along with the contraction shown in Figure 5, explains the reduction of viscosity at low temperature.

Conclusion

We have investigated the structure of an EP copolymer of 80 mol % ethylene content in two selective solvents, MCH and THN. In both solvents the polymer formed aggregates in the temperature range of -10 to 50°C . According to DLS-viscometry data, the aggregation number for both solutions at 0.100% concentration was 2000–4000 polymers per cluster, with a slight increase in aggregation number at lower temperatures. By comparison, SLS zero-angle intensity analysis at the same concentration showed that the aggregation varied from 10 polymers per cluster at 50°C in both solvents to several hundred polymers per cluster in MCH to several thousand in THN at -10°C . This discrepancy between SLS and DLS-viscometry results is probably due to polydispersity effects. Evaluation of concentrations ranging from 0.002% to 0.200% by DLS and SLS Zimm plots provided support for the picture of increased aggregation for the THN samples at -10°C . We speculate that clusters in MCH at all temperatures, and in THN at high temperatures, contained randomly distributed high ethylene content domains interspersed with solvated propylene-rich domains. Since the hydrodynamic radius of the THN samples was reduced at low temperatures, in conjunction with the increased aggregations, it is possible that the high ethylene content areas contracted further as the solvent quality became poorer. *This change in microstructure (contraction and aggregation) explains the drop in viscosity in THN at low temperature.* The MCH sample did not show this same trend since the hydrodynamic radius increased with increased aggregation. Thus, while intermolecular aggregation did occur, the solvent quality was not poor enough to cause contraction of the clusters and the polymer in this solvent did not exhibit any temperature-sensitive viscosity behavior. It is probable that at temperatures lower than -10°C (i.e., poorer solvent quality) a similar drop in specific viscosity would be observed in MCH.

Acknowledgment. This work was funded, in part, by a grant from the Texaco R & D Department.

References and Notes

- Booser, E. R. In *Encyclopedia of Chemical Technology*; Mark, H. F., Othmer, D. F., Overberger, C. G., Seaborg, G. T., Grayson, M., Eckroth, D., Eds.; Wiley Interscience: New York, 1982; Vol. 14.
- Rubin, I. D.; Sen, A. *J. Appl. Polym. Sci.* **1990**, *40*, 523.
- Mays, J. W.; Fetters, L. J. *Macromolecules* **1989**, *22*, 921.
- Maderek, E.; Wolf, B. A. *Angew. Makromol. Chem.* **1988**, *161*, 157.
- Filiatrault, D.; Phuong-Nguyen, H.; Delmas, G. *J. Polym. Sci.: Polym. Phys.* **1981**, *19*, 763.
- Filiatrault, D.; Delmas, G. *J. Polym. Sci.: Polym. Phys.* **1981**, *19*, 773.
- Filiatrault, D.; Delmas, G. *Macromolecules* **1979**, *12*, 65, 69.
- Delmas, G.; Daviet, V.; Filiatrault, D. *J. Polym. Sci.: Polym. Phys.* **1976**, *14*, 1629.
- Sen, A.; Rubin, I. D. *Macromolecules* **1990**, *23*, 2519.
- Rubin, I. D.; Stipanovic, A. J.; Sen, A. Presented at the SAE Fuels and Lubricants Meeting, Tulsa, October 1990, SAE Paper No. 902092.
- Sloniewsky, A. R.; Evans, G. T.; Anderson, P. *Polym. Sci., Part A-2*, **1968**, *6*, 1555.
- Dewalt, L. E.; Ou-Yang, H. D. *Mater. Res. Soc. Symp. Proc.* **1992**, *248*, 203.
- Einstein, A. *Ann. Phys.* (4), **1906**, *19*, 289; **1911**, *34*, 591.
- Schmitz, K. S. *An Introduction to Dynamic Light Scattering by Macromolecules*; Academic Press: San Diego, CA, 1990.
- Mandelkern, L.; Flory, P. J. *J. Chem. Phys.* **1952**, *20*, 212.
- Flory, P. J. *Statistical Mechanics of Chain Molecules*; Hanser: Munich, and Oxford University Press: New York, 1988.
- de Gennes, P. G. *Scaling Concepts in Polymer Physics*; Cornell University Press: Ithaca, NY, 1979.